

**VIETNAM NATIONAL UNIVERSITY, HANOI  
UNIVERSITY OF ENGINEERING AND TECHNOLOGY**



**PHAN HOANG ANH**

**RESEARCH AND DEVELOPMENT OF LAB  
ON A CHIP (LOC) DEVICE TO DETECT AND  
QUANTIFY LUNG CANCER CELLS**

**ABSTRACT OF PHD THESIS IN ELECTRONIC ENGINEERING**

**HANOI – 2025**

**VIETNAM NATIONAL UNIVERSITY, HANOI  
UNIVERSITY OF ENGINEERING AND TECHNOLOGY**



**PHAN HOANG ANH**

**RESEARCH AND DEVELOPMENT OF LAB  
ON A CHIP (LOC) DEVICE TO DETECT AND  
QUANTIFY LUNG CANCER CELLS**

**ABSTRACT OF PHD THESIS IN ELECTRONIC ENGINEERING**

**MAJOR :** ELECTRONIC ENGINEERING

**MAJOR CODE :** 9520203

**SUPERVISOR :** ASSOC. PROF. DR. NGUYEN HOANG HAI

**CO-SUPERVISOR :** PROF. DR. CHU DUC TRINH

**HANOI – 2026**

# Abstract

Cancer remains a leading cause of mortality worldwide, with lung cancer accounting for the highest proportion of cancer-related deaths. Early detection of circulating tumor cells (CTCs) is crucial for timely diagnosis, prognosis assessment, and treatment monitoring. However, CTCs are extremely rare in peripheral blood, with approximately one CTC per  $10^6$ – $10^7$  white blood cells, making their isolation and detection technically challenging. This thesis presents the development of an integrated Lab-on-a-Chip (LoC) platform for the isolation, detection, and counting of A549 lung cancer cells using a combination of magnetic separation, impedance measurement, and machine learning techniques.

The research objectives are: (1) to investigate and develop an integrated Lab-on-a-Chip platform by designing and fabricating a microfluidic device with optimized magnetic separation structures, and CTC detection and enumeration system; and (2) to experimentally validate the proposed system and systematically evaluate its performance in terms of capture efficiency, detection accuracy, and robustness under relevant operating conditions.

The proposed system employs superparamagnetic  $\text{Fe}_3\text{O}_4$  nanoparticles functionalized with EpCAM-specific aptamers for selective binding to A549 cancer cells. The microfluidic chip features a serpentine channel design with optimized trap regions that generate high magnetic field gradients under an external permanent magnet. An impedance measurement circuit based on lock-in amplification technique was developed to capture cellular impedance signals. Signal processing algorithms utilizing

peak detection and machine learning models were implemented for automated cell classification and counting.

Simulation results demonstrate capture efficiencies of 80%, 94%, and 100% for magnetic bead sizes of 1.36  $\mu\text{m}$ , 3.00  $\mu\text{m}$ , and 4.50  $\mu\text{m}$ , respectively. The fabricated microfluidic chip with channel dimensions of 30  $\mu\text{m}$  enables single-cell flow alignment for precise impedance measurement. The impedance measurement system successfully distinguishes cell signals characterized by bipolar peaks from background noise. Machine learning models, including IsolationForest and OneClassSVM, achieved classification accuracy exceeding 88% for cell signal recognition.

This thesis contributes to the field of cancer diagnostics by presenting a compact, cost-effective, and automated platform for CTC detection. The integration of magnetic separation, impedance sensing, and intelligent signal processing on a single microfluidic chip provides a promising approach for point-of-care cancer screening applications. Future work will focus on clinical validation with patient blood samples and further optimization of system sensitivity and specificity.

## **Summary of the Thesis Structure and Content**

### **Introduction**

The introduction presents the background and context of the research, emphasizing the increasing burden of cancer, particularly lung cancer. It identifies the detection of Circulating Tumor Cells (CTCs) as a critical but challenging task due to their rarity in blood. The thesis sets out to develop a microfluidic system inte-

grating magnetic separation and impedance measurement to isolate and analyze CTCs. The research objectives, scientific significance, and the structure of the dissertation are outlined.

## Chapter 1: Overview of the Research

Chapter 1 provides a comprehensive overview of the cancer situation and the mechanisms of metastasis. Figure 1.2 illustrates the metastatic process through circulating tumor cells (CTCs). During metastasis, tumor cells detach from the primary tumor and enter the circulatory system, thereby becoming circulating tumor cells. This process involves the epithelial-to-mesenchymal transition and marks the initial stage of metastasis.

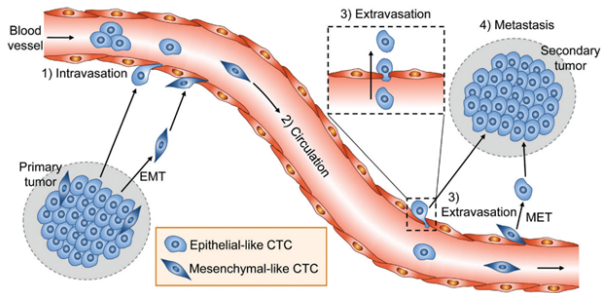


Figure 1.2: Diagram illustrating tumor metastasis via CTCs/CTM.

Figure 1.4 presents a block diagram of a CTC cell separation system utilizing magnetic nanoparticles and biological antibodies combined with microfluidic technology. The biochip structure comprises two parts: the first part separates white blood cells (WBCs) from the solution using a combination of magnetic

nanoparticles and antibodies that specifically recognize WBCs. The second part separates cells expressing the EpCAM membrane protein using EpCAM-specific antibodies.

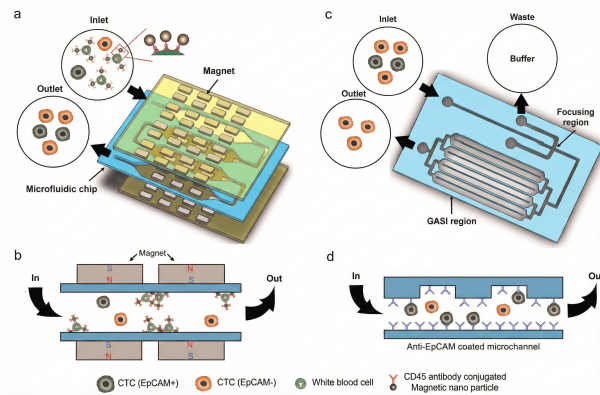


Figure 1.4: Block diagram of a CTC cell separation system utilizing magnetic nanoparticles and biological antibodies.

The thesis proposes a Lab-on-a-Chip system utilizing an integrated microfluidic chip platform. Figure 1.11 illustrates the integrated Lab-on-a-Chip platform for single-cell analysis, detailing the sequential operational stages: (a) Upstream magnetic trapping zone for selective enrichment of magnetically labeled CTCs. (b) Inertial microfluidic channel for cell ordering and spacing. (c) Cell encapsulation unit generating water-in-oil microdroplets at a T-junction. (d) Integrated electrode region for impedance-based detection of droplet contents. (e) Active microdroplet manipulation and sorting section. (f) Downstream sorting junction directing droplets into collection or waste outlets based on sensor feedback.

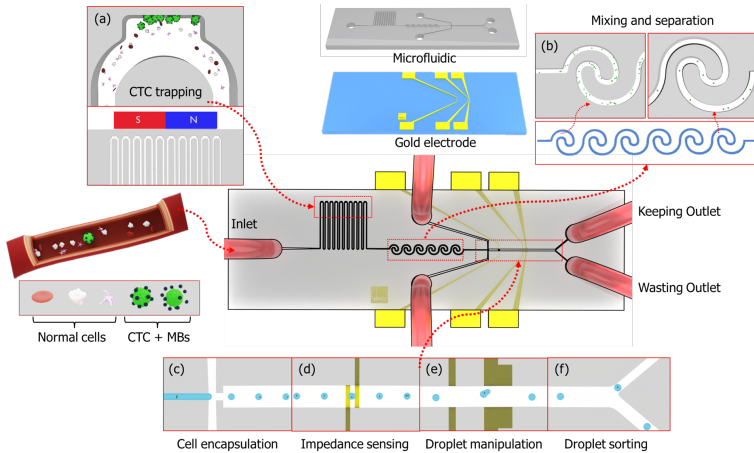


Figure 1.11: Schematic illustration of the integrated Lab-on-a-Chip platform for single cell analysis, detailing the sequential operational stages: (a) Upstream magnetic trapping zone for selective enrichment of magnetically labeled CTCs. (b) Inertial microfluidic channel for cell ordering and spacing. (c) Cell encapsulation unit generating water-in oil microdroplets at a T-junction. (d) Integrated electrode region for impedance-based detection of droplet contents. (e) Active microdroplet manipulation and sorting section. (f) Downstream sorting junction directing droplets into collection or waste outlets based on sensor feedback.

## Chapter 2: Theoretical Basis and Simulation

This chapter establishes the theoretical framework for the proposed methods. It details the mechanism of aptamer-magnetic particle binding, where  $\text{Fe}_3\text{O}_4$  nanoparticles are functionalized with EpCAM-specific aptamers to selectively target A549 lung cancer cells (Figure 2.1).

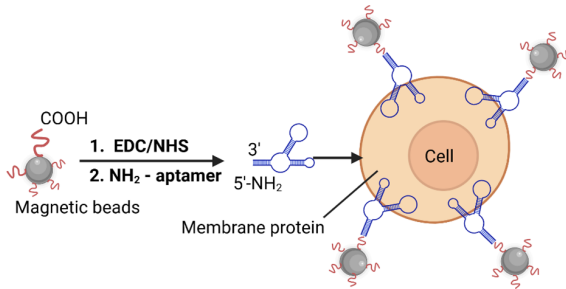


Figure 2.1: The adhesion of MB to the membrane proteins of the A549 target cells is mediated by the NH<sub>2</sub> aptamer.

The thesis proposes a cavity-integrated microchannel design (Figure 2.2) that utilizes magnetic forces to trap labeled cells in lateral chambers while allowing other blood components to pass. The channel dimensions are 100  $\mu\text{m}$  in width for the main channel, while the cavities extend to a length of 340  $\mu\text{m}$  and a width of 100  $\mu\text{m}$ .

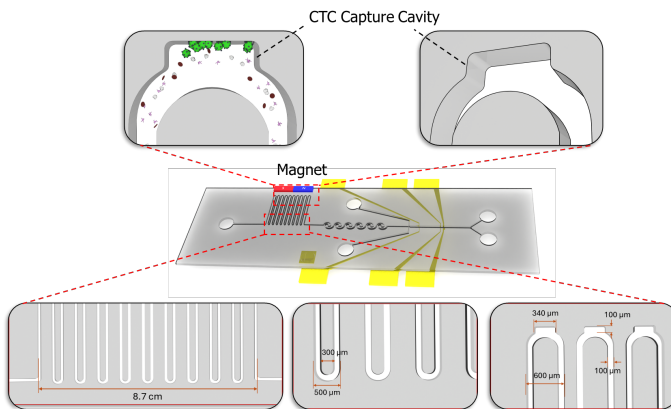


Figure 2.2: The proposed microfluidic system for CTC isolation in cavities. A. Schematic of the microfluidic device consisting of a channel pad placed on a glass substrate. The channel dimensions are  $100\ \mu\text{m}$  in width for the main channel, while the cavities (cell retention regions) extend to a length of  $340\ \mu\text{m}$  and a width of  $100\ \mu\text{m}$ .

To ensure the efficiency of downstream impedance-based cell counting, a continuous spiral inertial microfluidic structure is proposed (Figure 2.4). This structure leverages hydrodynamic forces for the effective focusing and spacing of the cell stream, utilizing a series of spiral loops with progressively decreasing dimensions.

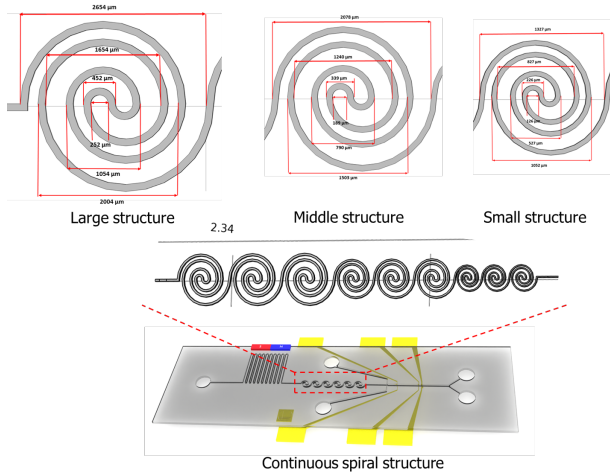


Figure 2.4: Proposed continuous spiral structure with progressively decreasing dimensions.

Figure 2.6 shows the microchannel structure for cell detection and counting using an integrated impedance sensor. The design includes electrodes to create differential measurement pairs, minimizing noise and optimizing accuracy.

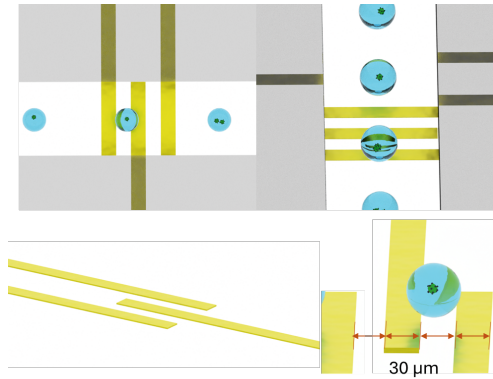


Figure 2.6: Microchannel structure for cell detection and counting using an integrated impedance sensor in a Lab-on-a-chip.

For droplet classification, the thesis presents a microfluidic droplet classification and separation device (Figure 2.8). The design incorporates gold electrode pairs subjected to different high and low DC voltages to achieve both steering and separation effects.

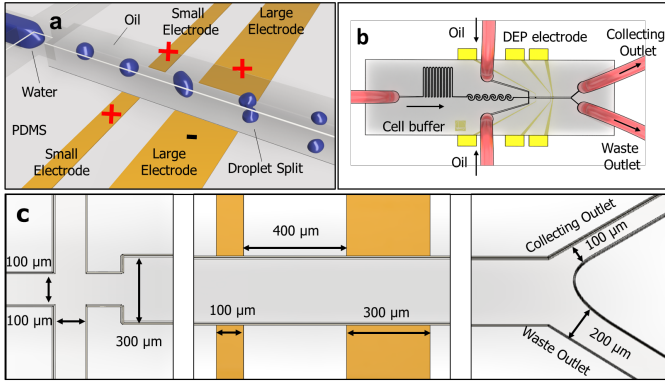


Figure 2.8: Microfluidic droplet classification and separation device. (a) Schematic illustration incorporating gold electrode pairs subjected to different high and low DC voltages with different sizes to achieve both steering and separation effects. (b) Water-in-oil structure designed to generate droplets through flow concentration effect with gold electrode pairs near the two outlets. (c) Dimensions of the inlet, outlet, main channel, and gold electrodes.

### Chapter 3: Material Preparation and Experiment Setup

Chapter 3 describes the experimental setup and material preparation. Figure 3.7 shows the image of the cell counting system setup, including key components such as a microscope, impedance measurement circuit, analysis computer, and camera.

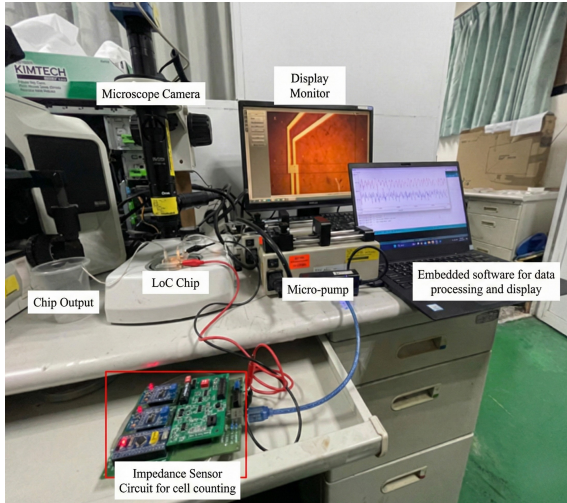


Figure 3.7: Image of the cell counting system setup.

Figure 3.8 shows the overall system for cell encapsulation in droplets and droplet sorting using DEP. The microfluidic chip has two input channels (oil and water solution) and one discharge channel.

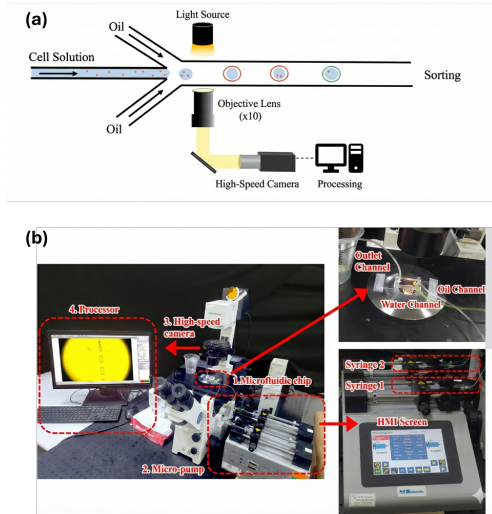


Figure 3.8: Overall system for cell encapsulation in droplets and droplet sorting using DEP.

To evaluate the binding efficiency of MBs on A549 lung cancer cells, the study proposed a method using a combination of object detection and semantic segmentation techniques (Figure 3.10).

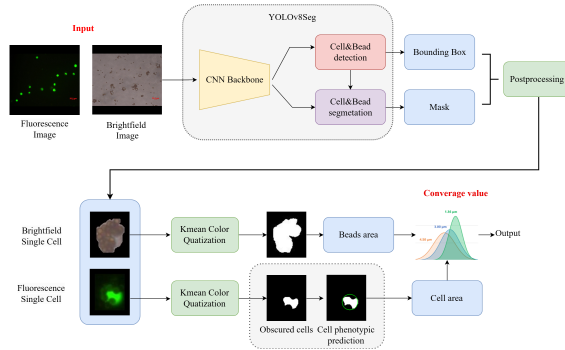


Figure 3.10: Schematic diagram of the detection and segmentation model for cells and magnetic particles.

## Chapter 4: Results and Discussion

Chapter 4 presents the results of the study. **Fabrication Results:** The microfluidic chip was successfully fabricated using PDMS technology. Figure 4.1 shows the fabricated chip with a  $30\ \mu\text{m}$  sensing channel, ensuring single-cell alignment for accurate impedance measurement.

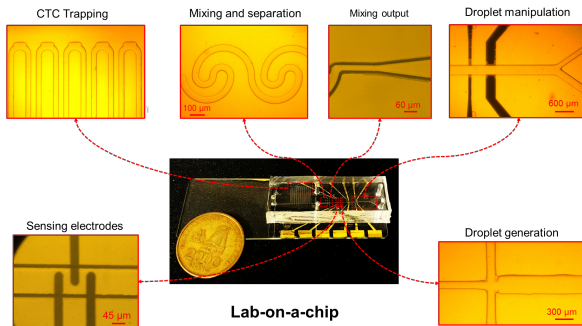


Figure 4.1: Results of the LoC chip after fabrication.

**Binding Results:** The results of the incubation and binding of immunomagnetic beads (IMBs) to the surface of A549 cancer cells are presented in Figure 4.11. The results show effective binding with magnetic particles of different sizes (1.36  $\mu\text{m}$ , 3.0  $\mu\text{m}$ , 4.5  $\mu\text{m}$ ).

	MBs-A549 cell conjugation images			Coverage range				
	Brightfield	Integration	Fluorescence					
Size of 1.36 $\mu\text{m}$								
Size of 3.00 $\mu\text{m}$								
Size of 4.50 $\mu\text{m}$								

Figure 4.11: Results of magnetic particle-A549 cell binding with different particle sizes (1.36  $\mu\text{m}$ , 3.0  $\mu\text{m}$ , 4.5  $\mu\text{m}$ ).

The study utilized a YOLOv8-based segmentation model to evaluate the binding efficiency. Figure 4.12 shows the segmentation results for cancer cells attached to 3.0  $\mu\text{m}$  and 4.5  $\mu\text{m}$  magnetic beads.

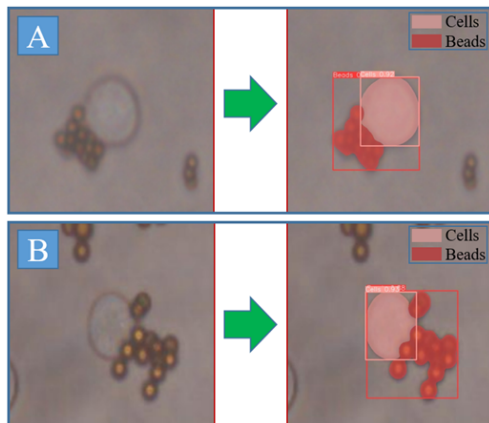


Figure 4.12: Yolov8 segmentation prediction. (A) Segmentation model with  $3.0 \mu\text{m}$  MB, (B) Segmentation model with  $4.5 \mu\text{m}$  MB.

The binding efficiency was further analyzed statistically. Figure 4.14 presents the distribution of coverage area for both bead sizes, showing that smaller beads ( $3.0 \mu\text{m}$ ) generally exhibit higher binding efficiency due to their larger surface-area-to-volume ratio.

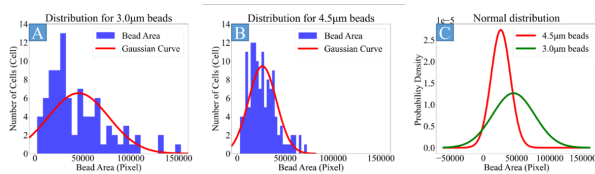


Figure 4.14: The binding efficiency of MBs during A549 cell recognition, represented as statistical graphs through the distribution of percentage coverage area values. (A) Distribution of the area of  $3.0\ \mu\text{m}$  MBs adhering to each cell. (B) Distribution of the area of  $4.5\ \mu\text{m}$  MBs adhering to each cell. (C) Gaussian curve illustrating the probability distribution of MBs in both cases.

To verify the capture efficiency in the microfluidic channel, experiments were conducted with stained cells. Figure 4.15 shows the capture of A549 cells (stained green) in the trapping cavities.

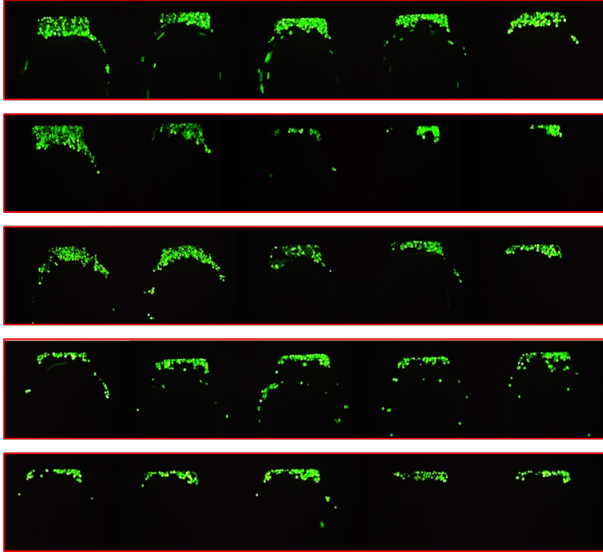


Figure 4.15: Results of A549 cells (stained green) being captured in the microfluidic channel.

**Droplet Formation:** The system’s ability to encapsulate cells in droplets was also evaluated. Figure 4.18 illustrates the droplet formation process at the T-junction.

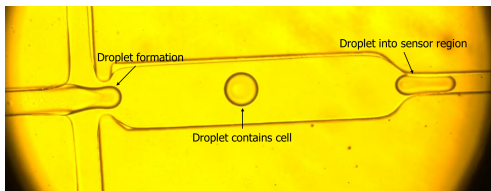


Figure 4.18: Results of droplet formation by the T-channel.

**Cell Counting Accuracy:** To quantify the accuracy of the impedance measurement system, a multi-step data processing and

validation procedure is performed. Figure 4.26 illustrates the cell counting system comprising electrodes and channel mold, along with raw data collected by the DAQ system and data after band-pass filtering.

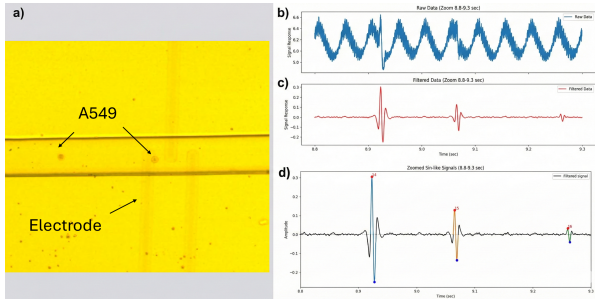


Figure 4.26: (a) Cell counting system comprising electrodes and channel mold. (b) Raw data collected by the DAQ system. (c) Data after bandpass filtering. (d) Filtered data magnified.

The study successfully demonstrated the isolation of A549 cells with high recovery rates and the classification of cell signals using machine learning algorithms with high accuracy.

## Conclusions and Future Work

This dissertation has presented a comprehensive study on the development of a microfluidic system for the isolation and analysis of Circulating Tumor Cells (CTCs). A novel microfluidic device integrating advanced separation techniques was successfully designed and fabricated. The system demonstrated high efficiency in isolating CTCs from blood samples, achieving high recovery rates and purity.

Numerical simulations provided valuable insights into the particle behavior within the microfluidic channels, validating the experimental results. The proposed method offers a label-free and low-cost alternative to existing commercial systems, making it suitable for potential clinical applications.

The main contributions of this dissertation can be summarized as follows:

1. A multifunctional microfluidic Lab-on-a-Chip system was integrated and successfully fabricated for the detection and counting of lung cancer cells. This platform incorporates magnetically assisted and inertial microfluidic separation, droplet-based single-cell encapsulation, impedance-based cell counting, and machine-learning-based signal processing, enabling automated, high-throughput analysis on a single chip.
2. New methods for cell detection, classification, and separation were proposed and experimentally validated, based on the combined use of electromagnetic techniques and image processing with machine learning models. These meth-

ods harness magnetic forces, non-uniform electric fields, impedance cytometry, and deep-learning-based image analysis to improve the sensitivity, selectivity, and reliability of lung cancer cell analysis.

While the results obtained in this study are promising, there are several avenues for future research to further improve the system and expand its applications. First, further optimization of the channel geometry and electrode configuration could enhance the throughput and sensitivity of the system.

Second, large-scale clinical trials with patient samples are necessary to validate the clinical utility of the device for cancer diagnosis and prognosis. Third, integrating the isolation module with downstream analysis capabilities, such as single-cell sequencing or drug screening, would provide a more comprehensive tool for cancer research. Finally, developing a fully automated and portable version of the system would facilitate its use in point-of-care settings.

## List of Publications Concerning the Dissertation

1. **Hoang Anh Phan**, Anh Thi Nguyen, Loc Do Quang, Tung Bui Thanh, Chun-Ping Jen, Trinh Chu Duc, “Image-based machine learning quantitative evaluation of bead-cell binding interaction”, (2025), *Sensors and Actuators A: Physical*, Vol. 367, 116123. (***Q1 Journal***)
2. **Hoang Anh Phan**, Kien Nguyen, Phong Tuan Pham, Loc Do Quang, Hang Bui Thu, Dang Bao Lam, Chun-Ping Jen, Tung Bui Thanh, Trinh Chu Duc, “On-demand electrostatic droplet sorting and splitting”, (2025), *Sensors and Actuators A: Physical*, Vol. 385, 116311. (***Q1 Journal***)
3. **Hoang Anh Phan**, Nguyen Dang Pham, Loc Quang Do, Tung Thanh Bui, Hai Hoang Nguyen, Trinh Duc Chu, “Machine learning-based bead enumeration in microfluidics droplets enhances the reliability of monitoring bead encapsulation toward single-cell sorting applications”, (2024), *Microfluidics and Nanofluidics*, Vol. 28, No. 8 (Article 71). (***Q2 Journal***)
4. **Hoang Anh Phan**, Loc Quang Do, Thanh Tung Bui, Thang Nguyen Van, Hoang Hai Nguyen, Trinh Chu Duc, “Automated detection and enumeration of bead encapsulation in microfluidic droplets based on deep learning”, (2024), *International Journal of Nanotechnology*, Vol. 21, No. 7-12, 609–621. (***Q4 Journal***)
5. **Hoang Anh Phan**, Anh Nguyen Thi, Nguyen Pham Dang,

Hien Vu-Dinh, Bao Lam Dang, Tung Thanh Bui, Chun-Ping Jen, Loc Do Quang, Hai Hoang Nguyen, Trinh Chu Duc, “Magnetic Bead Conjugated Lung Tumor Cell Binding Efficiency Assessment Based on Deep-Learning Approach”, (2023), *2023 1st International Conference on Health Science and Technology (ICHST)*, 1-6. (**Scopus Conference**)

6. **Hoang Anh Phan**, Nguyen Van Phu, Tung Le Thanh, Van Tan Duong, Anh Phuc Dao, Van Dai Pham, Loc Do Quang, Thanh Tung Bui, Duc Trinh Chu, “Machine Learning-based Single-cell Analysis Using Microfluidic Impedance Flow Cytometer”, (2025), *VNU Journal of Science: Mathematics - Physics*, Vol. 41, No. 2. (**VNU Journal**)